chemosensors

MDPI

Communication

A Bioorthogonal Double Fluorogenic Probe to Visualize Protein–DNA Interaction

Attila Kormos [1], Alexandra Egyed [1,2], Jasmine M. Olvany [1], Ágnes Szatmári [1], Adrienn Biró [1], Zsóka Csorba [1], Péter Kele [1,*] and Krisztina Németh [1,*]

[1] Chemical Biology Research Group, Institute of Organic Chemistry, ELKH Research Centre for Natural Sciences, Magyar Tudósok Krt 2, 1117 Budapest, Hungary; kormos.attila@ttk.hu (A.K.); egyed.alexandra@ttk.hu (A.E.); jasmine.olvany@case.edu (J.M.O.); szatmari.agnes@ttk.hu (Á.S.); biro.adrienn@ttk.hu (A.B.); csorba.zsoka@ttk.hu (Z.C.)

[2] Hevesy György PhD School of Chemistry, Eötvös Loránd University, Pázmány Péter Sétány 1/a, 1117 Budapest, Hungary

* Correspondence: kele.peter@ttk.hu (P.K.); nemeth.krisztina@ttk.hu (K.N.)

Abstract: Two sets of bioorthogonally applicable, double fluorogenic probes, capable of sensing DNA–protein interactions, were prepared by installing an azide or tetrazine motif onto structurally fluorogenic, DNA sensitive frames. Installation of these bioorthogonal functions onto DNA intercalating dyes furnished these scaffolds with reactivity based fluorogenicity, rendering these probes double-fluorogenic, AND-type logic switches that require the simultaneous occurrence of a bioorthogonal reaction and interaction with DNA to trigger high intensity fluorescence. The probes were evaluated for double fluorogenic behavior in the presence/absence of DNA and a complementary bioorthogonal function. Our studies revealed that azide and tetrazine appending thiazole orange frames show remarkable double fluorogenic features. One of these probes, a membrane permeable tetrazine modified thiazole orange derivative was further tested in live cell labeling studies. Cells expressing bioorthogonalized DNA-binding proteins showed intensive fluorescence characteristics of the localization of the proteins upon treatment with our double fluorogenic probe. On the contrary, labeling similarly bioorthogonalized cytosolic proteins did not result in the appearance of the fluorescence signal. These studies suggest that such double-fluorogenic probes are indeed capable of sensing DNA–protein interactions in cells.

Keywords: double fluorogenic sensor; thiazole orange; bioorthogonal labeling; DNA intercalator; protein–DNA interaction; confocal imaging; self-labeling tag

check for updates

Citation: Kormos, A.; Egyed, A.; Olvany, J.M.; Szatmári, Á.; Biró, A.; Csorba, Z.; Kele, P.; Németh, K. A Bioorthogonal Double Fluorogenic Probe to Visualize Protein–DNA Interaction. *Chemosensors* **2022**, *10*, 37. https://doi.org/10.3390/chemosensors10010037

Academic Editor: Bolze Frederic

Received: 17 December 2021
Accepted: 13 January 2022
Published: 17 January 2022

Publisher's Note: MDPI stays neutral with regard to jurisdictional claims in published maps and institutional affiliations.

Copyright: © 2022 by the authors. Licensee MDPI, Basel, Switzerland. This article is an open access article distributed under the terms and conditions of the Creative Commons Attribution (CC BY) license (https://creativecommons.org/licenses/by/4.0/).

1. Introduction

DNA–protein interactions are essential to many of the basic mechanisms of life, such as transcription, replication, gene activation/silencing, DNA packaging, or gene editing. The central role of these processes in cell functioning, maturation, differentiation, or in tumorigenesis calls for methods that allow us to obtain improved insight into these events at the biomolecular level. These needs have placed the *in cellulo* sensing of specific DNA–protein interactions into the focus of chemical biology research. To date, several methods have emerged to study nucleic acid–protein interactions. Chromatin immunoprecipitation (ChIP) [1] based methods are suitable for capturing snapshots of DNA–protein interactions in live cells with in vitro work-up and detection. Others, i.e., electrophoretic mobility shift assays (EMSA) [2] or pull-down assays [3], provide the means to detect low abundance proteins in lysates. Further instances have applied the intercalating dye, thiazole orange (TO), which was covalently attached to DNA binding proteins (a zinc finger containing glucocorticoid receptor [4] or histone protein [5]) for the fluorescent detection of DNA–protein interactions *in vitro*. Reporter assays [6] provide an indirect way to track down protein (e.g., transcription factor)—DNA interaction via real-time monitoring of

translational activity of a promoter DNA sequence coding for the target promoter protein fused to a reporter gene that encodes a protein with detectable properties (e.g., fluorescent protein). Other approaches employ oligonucleotides tagged with a probe sensitive to protein binding [7,8]. Such tagging can be carried out post-synthetically or by means of non-canonical building blocks modified with an environmentally (e.g., polarity, viscosity) sensitive motif [9]. Non-canonical nucleotides can be incorporated into DNA synthetically (e.g., on solid phase) or by means of metabolic incorporation or primer extension (PEX) [10]. The changes in fluorescence due to the altered microenvironment upon protein binding are then correlated with the DNA–protein interaction. The pioneering work of Hocek and co-workers [11,12] has resulted in several probe-appending nucleosides capable of sensing DNA–protein interactions. In one of their latest reports, they describe aminophenyl- or aminonaphthyl-methoxychromone modified nucleosides that show a moderate increase in fluorescence and a remarkable change in emission color at the same time [13]. In an earlier report, Seio et al. [14] reported on a benzofurane appending nucleoside that allowed a ca. 100-fold increase upon its interaction with a single-strand binding protein. Although the above examples are suitable to detect DNA–protein interactions mostly in vitro, there are no viable methodologies with the ability to visualize the ever-changing relationship between protein and DNA in live cells.

The methods that utilize environment sensitive fluorescent probes described above generally depend on the covalent modification of DNA building blocks. The incorporation of non-canonical nucleotides into DNA is possible through solid phase synthesis or PEX, but these modified DNAs are still considered extrachromosomal when delivered into cells. Chromosomal incorporation of non-canonical nucleotides can occur when the desired base is tolerable to enzymatic machinery; however, the insertion of these is non-specific and general. Neither of these cases allow for specific targeting of protein–DNA interaction at focused places. When there is a specific interaction with a protein of interest (POI), manipulation can be achieved site-specifically at both termini, e.g., with small self-labeling enzyme tags, or virtually at any positions with minimally perturbing non-canonical amino acids (ncAAs) via the extension of the genetic code [15–20]. Such genetic incorporation of, e.g., bioorthogonalized ncAAs, enable site-specific fluorescent tagging. Our continuing efforts to develop bioorthogonally applicable, fluorogenic probes highlighted the viability of an azide- or tetrazine-based modulation of fluorescence properties. Several examples proved that both bioorthogonal functions are suitable for the efficient quenching of the fluorescence of probes [21–24].

The above considerations and challenges prompted us to design and synthesize a set of bioorthogonally functionalized environment sensitive probes that combine the reactivity-based fluorogenicity of an azide or tetrazine bearing scaffold with the structural fluorogenicity of DNA probes. We hypothesized that such double-fluorogenic probes require the simultaneous events of a covalent conjugation to a site specifically bioorthogonalized POI and interaction with DNA to fully restore fluorescence (Scheme 1). Such probes are anticipated to be suitable to indicate DNA–protein interaction in a cellular environment using confocal microscopy imaging.

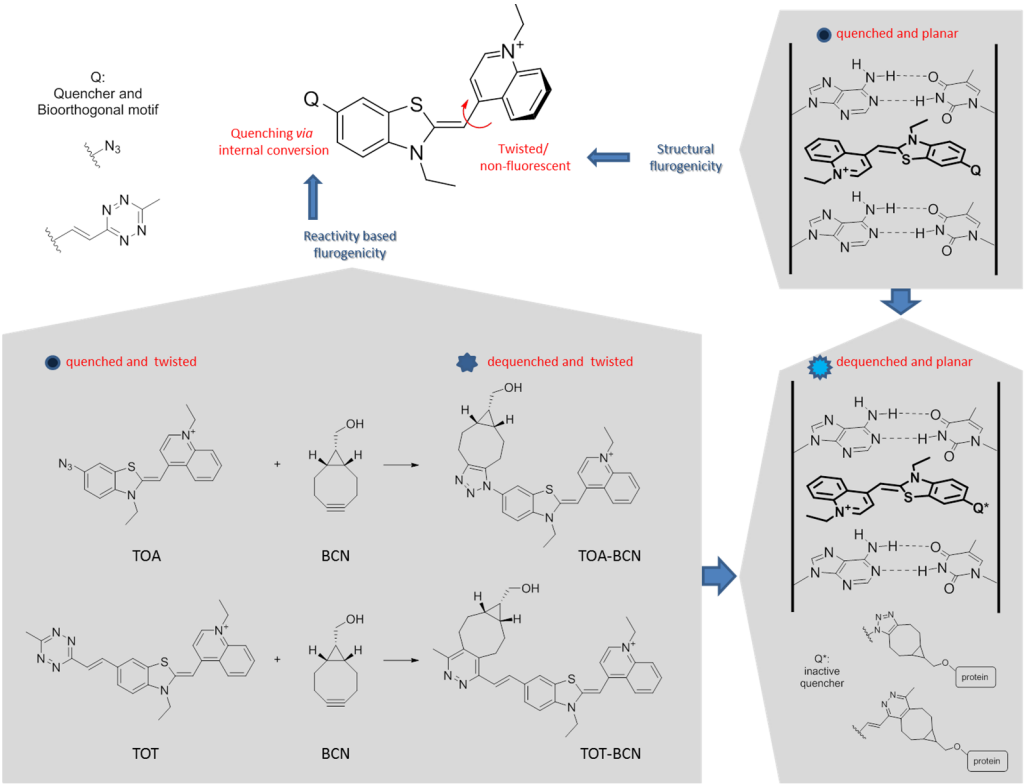

Scheme 1. Proposed AND-type double fluorogenicity of bioorthogonally functionalized environment sensitive probes. Thiazol orange azide (**TOA**) and tetrazine (**TOT**) are representatives of these DNA sensors showing reactivity (quenched and dequenched states) and structural (twisted and planar conformations) based fluorogenicities.

2. Materials and Methods

Experimental details, synthetic procedures, spectroscopic characterization, physical data determination, details on the cell imaging experiments, further images, and the viability assessment can be found in the Supplementary Materials.

3. Results and Discussion

3.1. Synthesis and Fluorogenic Evaluation of Probes

We chose four structurally fluorogenic DNA probe frames [25–28] to be modified with an azide motif. The selection of the dye-frames was based on their spectral properties, synthetic accessibility, and modifiability (Figure 1). The plain probes, together with their azide modified congeners, were accessed through convergent synthetic routes (Scheme S1).

With the probes in hand, we next assessed their fluorogenic features by measuring the fluorescence intensities of the probes in the absence or presence of a complementary bioorthogonal motif (i.e., a cyclooctyne, (1R,8S,9s)-bicyclo [6.1.0] non-4-yn-9-ylmethanol, BCN) (Scheme S4), and DNA in a buffered medium (Tris-PBS 1:4). For comparison, we also measured the fluorescence of non-bioorthogonalized parent frames under similar conditions. In general, most of the non-bioorthogonalized probes exhibited negligible fluorescence in the absence of DNA and an enhanced signal in the presence of nucleic acids. **TO***, on the other hand, showed a negligible effect in the presence of nucleic acids, pointing out the importance of the substitution pattern on intercalation or structural constriction.

Installation of an azide function onto the structurally fluorogenic frameworks generally resulted in quenched fluorescence even in the presence of DNA (Figure 2, Tables 1, S1 and S2). The combined addition of BCN and DNA, on the other hand, resulted in increased emission intensities. Evaluation of the results revealed that **TOA** possesses remarkable double fluorogenic features. Although synthetic accessibility of organic azides is quite appealing, the copper-free, strain-promoted cycloaddition reactions of azides and cyclooctynes suitable

for live cell applications have limited reaction rates, requiring either extended reaction times or higher probe loading [29]. Indeed, when we measured the conversion percentage of the reaction of **TOA** and BCN, a 90% conversion could be detected after 10 h (Figure S1).

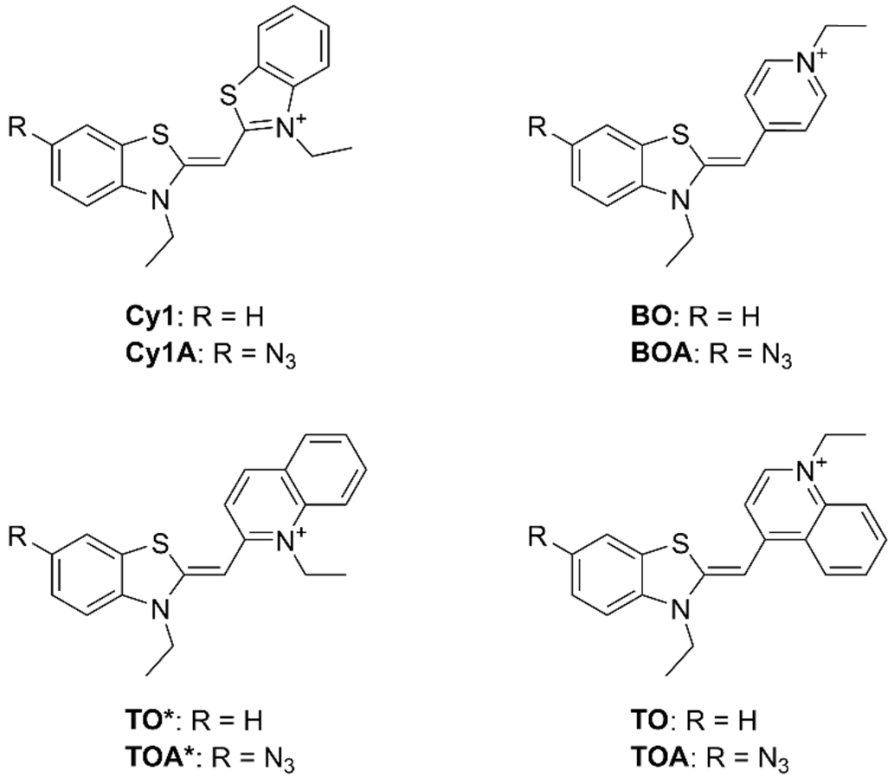

Figure 1. Structures of **Cy1, BO**, **TO*,** and **TO** frames, and their azide modified derivatives.

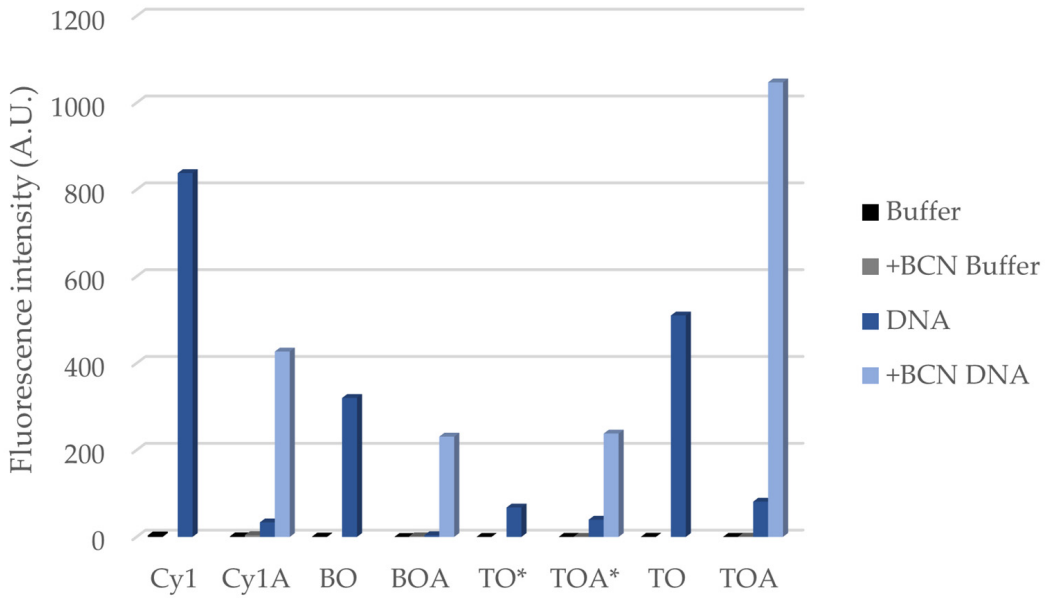

Figure 2. Fluorescence intensities of 1.0 μM **Cy1, BO**, **TO*,** and **TO** frames, their azide modified derivatives, and the BCN conjugates of the azides in the absence and presence of 0.4 mg/mL calf thymus dsDNA in TRIS–PBS 1:4 at 21 °C. λ_{exc}: 405 nm for Cy1, 420 nm for **BO**, 460 nm for **TO***, and 480 nm for **TO** derivatives, the emission was recorded at the maxima.

Table 1. Fluorescence quantum yields of **Cy1, BO**, **TO***, and **TO** frames, their azide modified derivatives, and the BCN conjugates of the azides in the absence and presence of DNA.

	Φ_{PBS}	+BCN Φ_{PBS}	Φ_{DNA}	+BCN Φ_{DNA}
Cy1	0.0028	-	0.41	-
Cy1A	0.0014	0.0028	0.047	0.19
BO	0.00053	-	0.24	-
BOA	N.D. [a]	0.0010	0.017	0.094
TO*	0.00013	-	0.050	-
TOA*	0.00021	0.00046	0.030	0.16
TO	0.00029	-	0.30	-
TOA	0.00033	0.00061	0.083	0.53

[a] Fluorescence could not be detected.

In order to avoid extended labeling times with the live cells, we explored the possibility of replacing the azide with the synthetically less accessible tetrazine as a quencher and bioorthogonal handle. At the same time, we involved further frames with red-shifted excitation/emission spectra. To this end, we have designed TO-derived (**TOT**) and cyanine-styrene-based scaffolds (**StyT1**, **StyT2**), as presented in Figure 3.

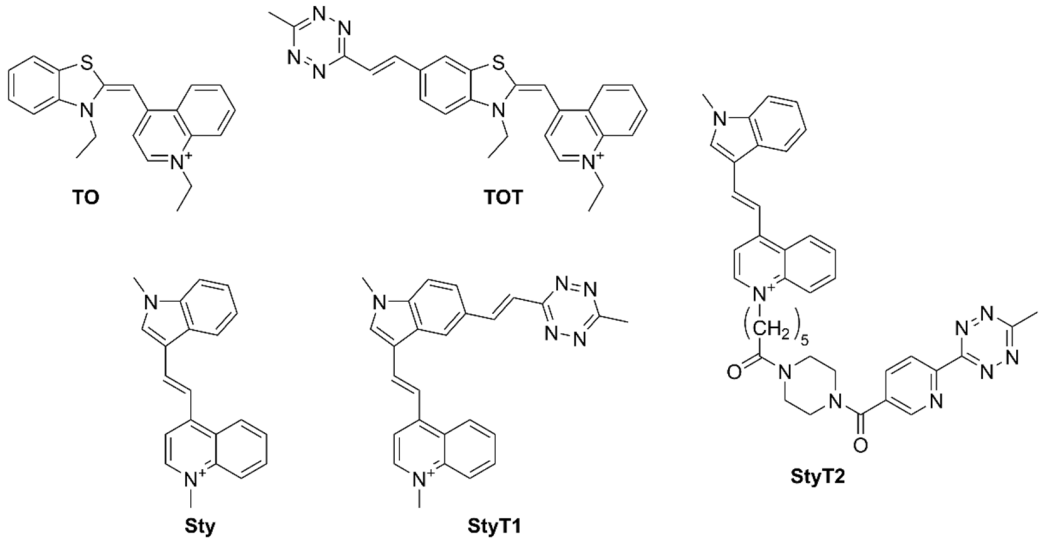

Figure 3. The structures of **TO** and **Sty** frames and their tetrazine modified derivatives.

Tetrazines can exert their quenching through various pathways. Through-bond energy transfer (TBET) [30] is believed to be the major mechanism, where the tetrazine is connected to the fluorescent frame via a conjugatable but electronically decoupled (twisted) linker. Förster resonance energy transfer is reported to be the main path of quenching, where the tetrazine and the fluorophore are connected through a flexible linker [31]. Finally, tetrazines that are directly conjugated to a fluorophore are reported to quench fluorescence by opening non-radiative relaxation pathways via internal conversion [32,33].

TOT and **Sty1** links the tetrazine via a conjugating vynilene motif, while **StyT2** carries the tetrazine through a flexible linker. We assumed that the quenching will be effected via internal conversion in the case of **TOT** and **StyT1,** while FRET is expected to be the main cause of quenching in the case of **StyT2**.

These tetrazine modified environment sensitive scaffolds were accessed via routine synthetic steps as presented in Schemes S2 and S3. In the same manner as for the azide motifs, we assessed the fluorogenicity of the probes and their parent frames in the presence/absence of BCN, and DNA (Figure 4, Tables 2, S1 and S2).

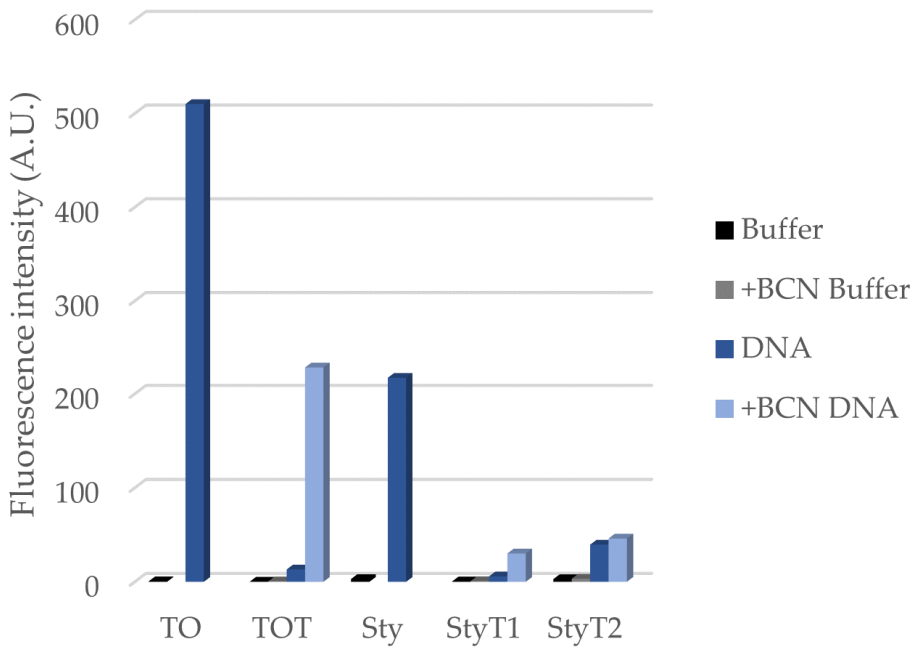

Figure 4. Fluorescence intensities of 1.0 μM **TO** and **Sty** frames, their tetrazine modified derivatives, and the BCN conjugates of the tetrazines in the absence and presence of 0.4 mg/mL calf thymus dsDNA in TRIS–PBS 1:4 at 21 °C. λ_{exc}: 480 nm for unsubstituted **TO** and 490 nm for all of the other probes, the emission was recorded at the maxima.

Table 2. Fluorescence quantum yields of **TO** and **Sty** frames, their tetrazine modified derivatives, and the BCN conjugates of the tetrazines in the absence and presence of DNA.

	Φ_{PBS}	+BCN Φ_{PBS}	Φ_{DNA}	+BCN Φ_{DNA}
TO	0.00029	-	0.30	-
TOT	N.D. [a]	0.0016	0.014	0.24
Sty	0.0031	-	0.19	-
StyT1	0.00093	0.0024	0.014	0.072
StyT2	0.014	0.013	0.15	0.15

[a] Fluorescence could not be detected.

Similarly to its azide derivative, **TOT** displayed significant double fluorogenicity. The **Sty** scaffold showed excellent fluorogenicity in good accordance with its original report [34]. Tetrazine modification via direct conjugation at the indole-ring (**StyT1**) or through a flexible linker appending at the quinolinium unit (**StyT2**), however, resulted in considerably lower fluorogenic performance, compared to the parent **Sty**. As expected, the qualitative assessment of the reaction rate showed much faster kinetics, as the cycloaddition of **TOT** with BCN (Scheme S4) went to completion within 2 h (Figure S2). **TOT** was then selected for cellular labeling studies.

3.2. Cellular Studies

To explore the DNA–protein sensory potential of **TOT** in the more challenging environment of live cells, we assessed the cytotoxicity of our bifunctional probe **TOT** on a HEK293T cell culture. The cells were treated with **TO** and **TOT** in the concentration range of 1–10 μM. Following a 24-h incubation period we performed an MTT test. TO exhibited a significant cytotoxic effect due to its strong intercalation activity. On the contrary, **TOT** did not affect cell viability substantially (Figure S3). This difference likely arises from the decreased intercalation activity of **TOT** due to the structural modification with the tetrazine unit.

Next, we wanted to demonstrate the ability of **TOT** to specifically sense protein–DNA interaction in cells. Therefore, we selected LaminA [35,36] and H2B [37,38] nuclear proteins as model POIs for the live cell labeling and imaging experiments. Intermediate filaments of LaminA polymerize into fibers to provide a complex meshwork in the inner surface of the nuclear membrane. Based on its structure and localization, it provides a platform for anchoring proteins and gives mechanical stability to the nucleus; furthermore, it has a pivotal role in higher order genome organization, chromatin regulation, the replication and repair of DNA and even transcription. Histone protein, H2B, plays an active role in the formation of nucleosomes, the basic units of DNA coiling. Their central character in chromatin organization, and transcription regulation is unquestionable. Their post-translational modification, methylation/demethylation, etc., are involved in epigenetic modulations as well. To install a complementary bioorthogonal function onto DNA-binding proteins, the C-termini of LaminA and H2B were fused with a self-labeling enzyme tag, HaloTag.

Cells expressing either LaminA-HaloTag or H2B-HaloTag proteins were treated with a cyclooctyne bearing the HaloTag substrate, HaloBCN (Scheme 2) [39]. The bioorthogonalized proteins were then treated with **TOT**. Following the incubation time, the cells were washed and fixed, then subjected to confocal microscopy. The microscopy images showed bright structured fluorescence, characteristics of the LaminA, and H2B localization (Figure 5). These experiments proved that (i) **TOT** is membrane permeable and (ii) it is able to sense protein–DNA interaction. In order to unquestionably prove that we sense DNA–protein interaction, non-DNA-binding cytoplasmic proteins were studied as well. To this end, cytosolic intermediate filament Vimentin [40] and an outer membrane protein of mitochondria (TOMM20) [41,42] were also fused to HaloTag at their C-termini (the C-terminus of TOMM20 is located in the cytosolic region, preventing interference with mitochondrial DNA). Similarly to the previous labeling experiments, we treated Vimentin-HaloTag or TOMM20-HaloTag expressing cells with HaloBCN first, then washed them and allowed them to react with **TOT**. Following washing and fixation, the cells were subjected to confocal microscopy imaging. To our delight, no fluorescence signal could be detected at the location of the proteins, presumably due to the lack of nucleic acid interaction (Figure 5).

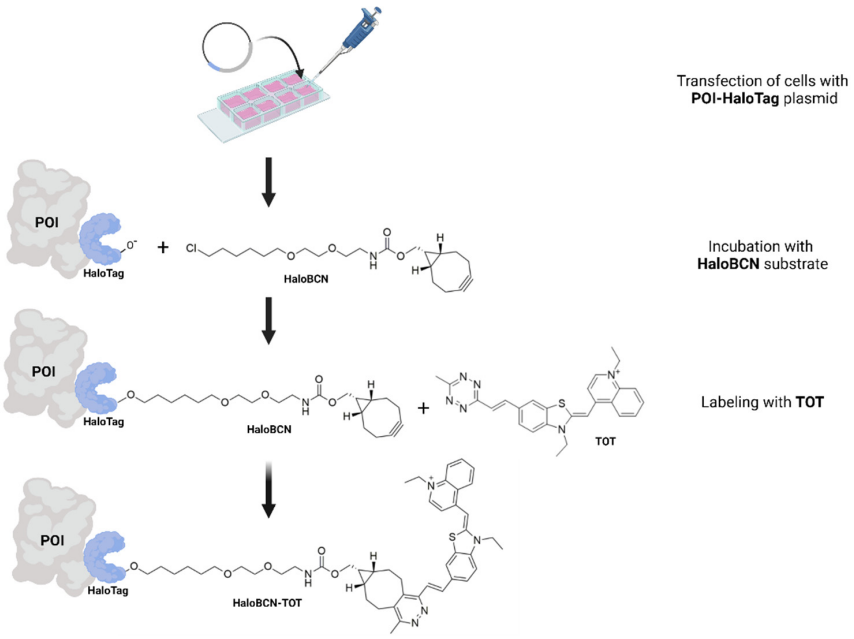

Scheme 2. The workflow of biorthogonal labeling with thiazole orange tetrazine (**TOT**). Transfected cells expressing the POI-HaloTag fusion protein are sequentially treated with HaloBCN substrate and **TOT**. Created with BioRender.com, (accessed on 10 December 2021).

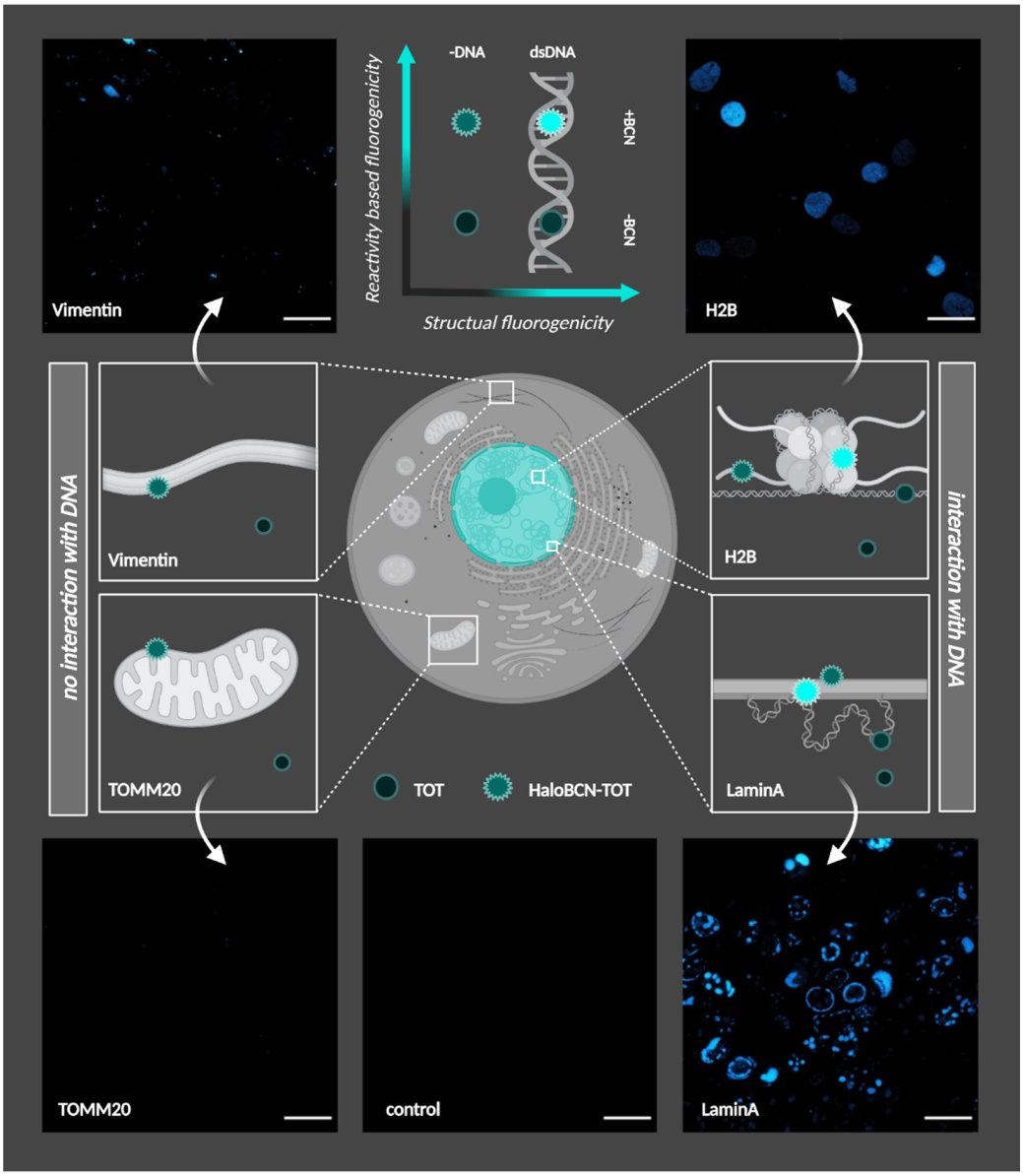

Figure 5. Confocal microscopy images of transfected HEK293T cells expressing the DNA interacting nuclear proteins H2B-HaloTag (**top, right**) or LaminA-HaloTag (**bottom, right**) and the non-DNA interacting cytosolic proteins Vimentin-HaloTag (**top, left**) and TOMM20-HaloTag (**bottom, left**) after treatment with HaloBCN (3 µM) and **TOT** (6 µM). The color calibration code shows the fluorescence intensity levels of **TOT** (**top, middle**). The control image refers to **TOT**-treated non-transfected cells (**bottom, middle**). Spectral detection: λ_{exc}: 488 nm/λ_{em}: 500–800 nm; Scale bar = 25 µm. Created with BioRender.com, (accessed on 10 December 2021).

These results indicate that the bioorthogonal reaction with BCN alone is not sufficient to trigger intense fluorescence and the presence of DNA in close proximity is also necessary. Control labeling of Vimentin-HaloTag or TOMM20-HaloTag with a non-DNA binding, fluorogenic tetrazine-probe (**SiR-Tet**, Figure S4) [43] showed that both proteins express the self-labeling tag (Figure 6).

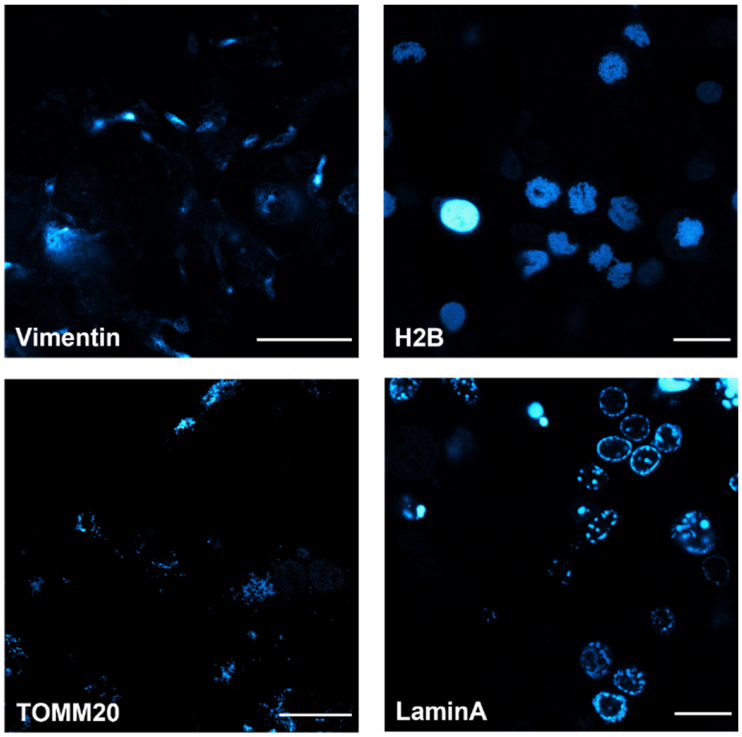

Figure 6. Confocal microscopy images of Vimentin-HaloTag, H2B-HaloTag, TOMM20-HaloTag and LaminA-HaloTag, expressing HEK293T cells treated with HaloBCN (3 μM) and **SiR-Tet** (3 μM) Spectral detection: λ_{exc}: 638 nm/λ_{em}: 650–800 nm; Scale bar = 25 μm.

4. Conclusions

In this study, we have explored the viability of bimodal chemosensors in order to address the great challenge of cellular sensingof DNA–protein interactions. Towards these aims, we have designed and synthesized two sets of bioorthogonally modified DNA sensitive, structurally fluorogenic frameworks in order to create double-fluorogenic AND-type logic switches. The installation of an azide or tetrazine function to these structurally fluorogenic frames furnished them with reactivity based fluorogenicity, thus requiring the simultaneous occurrence of a bioorthogonal reaction and interaction with DNA to trigger high intensity fluorescence. We have elaborated the two sets of such azide or tetrazine based probes for double fluorogenic behavior and found that, in both sets, the thiazole orange frame gives the best performance in terms of fluorescence increase. We then applied the membrane permeable tetrazine appending thiazole orange (**TOT**) to live cells expressing proteins bearing the complementary bioorthogonal function (BCN). Confocal microscopy studies showed that in the case of the DNA-interacting proteins, LaminA or H2B, an intense fluorescence appeared, in accordance with the localization of the proteins. This finding is further supported by the lack of detectable fluorescence of the two control cytosolic proteins, Vimentin and TOMM20.

These studies indicate that our double fluorogenic (i.e., reactivity-based- and structural-fluorogenicity) probes are indeed suitable for cellular sensing of DNA–protein interactions. Moreover, unlike other attempts to sense DNA–protein interactions using fluorogenic DNA building blocks, our approach allows protein-specific and site-specific incorporation of the probes. Such protein modifications are possible via fusion tags, as used in this work, or via genetic incorporation of non-canonical amino acids, leading to minimally perturbed modifications. Although this proof-of-concept study confirms the viability of such probes, their use, e.g., in gene-expression or epigenetic studies, requires further improvements, such as screening for more photostable frames, or conformational studies of structures to achieve optimized binding between the POI and DNA.

Supplementary Materials: The following supporting information can be downloaded at: https://www.mdpi.com/article/10.3390/chemosensors10010037/s1, Details of synthetic procedures, characterization, spectroscopy, and cellular studies. Scheme S1. (a) Et_3N, EtOH, 75 °C, 60 min (b) Et_3N, CH_2Cl_2, rt, 16 h. Scheme S2. (a) 1. $NaNO_2$, HCl, H_2O, 0 °C, 10 min, 2. KI, 40 °C, 20 min, (b) $(EtO)_2SO_2$, 100 °C, 16 h, (c) N-ethyl-4-methyl-quinolinium iodide, Et_3N, CH_2Cl_2, rt, 16 h, (d) 2-(6-methyl-1,2,4,5-tetrazin-3-yl)ethyl methanesulfonate, $Pd_2(dba)_3$, QPhos, Cy_2NMe, DMF, 100 °C MW, 60 min. Scheme S3. (a) piperidine, EtOH, Δ, 16 h for **Sty** and **4**, 60 min for **5**, (b) 2-(6-methyl-1,2,4,5-tetrazin-3-yl)ethyl methanesulfonate, $Pd_2(dba)_3$, QPhos, Cy_2NMe, DMF, 100 °C MW, 60 min, (c) Boc-piperazine, HATU, iPr_2NEt, CH_2Cl_2, rt, 30 min, (d) TFA, CH_2Cl_2, rt, 20 min, (e) 6-(6-methyl-1,2,4,5-tetrazin-3-yl)nicotinic acid, HOBt, HBTU, iPr_2NEt, MeCN, rt, 60 min. Scheme S4. Representative reactions of azides and tetrazines with BCN using **TOA** and **TOT** as examples. Table S1. Absorption maxima and molar extinction coefficients at the absorption maxima of the dyes in the presence or absence of BCN and DNA. Table S2. Emission maxima and fluorescence quantum yields of the dyes in the presence or ab-sence of BCN and DNA. Figure S1. Conversion of the cycloaddition reaction of **TOA** and BCN as a function of time. Figure S2. Conversion of the cycloaddition reaction of **TOT** and BCN as a function of time. Figure S3. Viability of HEK293T cells upon treatment of **TO** and **TOT** in the percentage of untreated controls (n = 3). Figure S4. Structure of SiR-tet.

Author Contributions: Conceptualization, A.K., P.K. and K.N.; methodology, A.K. and K.N.; investigation, A.K., A.E., J.M.O., Á.S., A.B., Z.C. and K.N.; writing—original draft preparation, K.N.; writing—review and editing, A.K., P.K. and K.N.; visualization, Z.C.; funding acquisition, A.K. and P.K. All authors have read and agreed to the published version of the manuscript.

Funding: This work has been implemented with the support provided by the Ministry of Innovation and Technology of Hungary from the National Research, Development and Innovation Fund, and financed under the [NKFIH-K-131439 and NKFIH-FK- 137589] funding schemes. We are also grateful for the generous support of the Eötvös Loránd Research Network (KEP-10). A.K. is grateful for the support of the Hungarian Academy of Sciences (BO/00154/21/7 János Bolyai Research Scholarship).

Data Availability Statement: Data available in the Supplementary Materials.

Conflicts of Interest: The authors declare no conflict of interest.

References

1. Furey, T.S. ChIP–seq and beyond: New and improved methodologies to detect and characterize protein–DNA interactions. *Nat. Rev. Genet.* **2012**, *13*, 840–852. [CrossRef]
2. Hellman, L.M.; Fried, M.G. Electrophoretic mobility shift assay (EMSA) for detecting protein–nucleic acid interactions. *Nat. Protoc.* **2007**, *2*, 1849–1861. [CrossRef] [PubMed]
3. Chaparian, R.R.; van Kessel, J.C. Promoter Pull-Down Assay: A Biochemical Screen for DNA-Binding Proteins. In *Stem Cell Renewal and Cell-Cell Communication*; Turksen, K., Ed.; Springer: New York, NY, USA, 2020; Volume 2346, pp. 165–172. [CrossRef]
4. Thompson, M.; Woodbury, N.W. Fluorescent and Photochemical Properties of a Single Zinc Finger Conjugated to a Fluorescent DNA-Binding Probe. *Biochemistry* **2000**, *39*, 4327–4338. [CrossRef] [PubMed]
5. Babendure, J.; Liddell, P.A.; Bash, R.; LoVullo, D.; Schiefer, T.K.; Williams, M.; Daniel, D.C.; Thompson, M.; Taguchi, A.K.W.; Lohr, D.; et al. Development of a fluorescent probe for the study of nucleosome assembly and dynamics. *Anal. Biochem.* **2003**, *317*, 1–11. [CrossRef]
6. Neefjes, M.; Housmans, B.A.C.; van den Akker, G.G.H.; van Rhijn, L.W.; Welting, T.J.M.; van der Kraan, P.M. Reporter gene comparison demonstrates interference of complex body fluids with secreted luciferase activity. *Sci. Rep.* **2021**, *11*, 1359. [CrossRef]
7. Valuchova, S.; Fulnecek, J.; Petrov, A.P.; Tripsianes, K.; Riha, K. A rapid method for detecting protein-nucleic acid interactions by protein induced fluorescence enhancement. *Sci. Rep.* **2016**, *6*, 39653. [CrossRef]
8. Song, D.; Graham, T.G.W.; Loparo, J.J. A general approach to visualize protein binding and DNA conformation without protein labelling. *Nat. Commun.* **2016**, *7*, 10976. [CrossRef]
9. Hocek, M. Enzymatic Synthesis of Base-Functionalized Nucleic Acids for Sensing, Cross-linking, and Modulation of Protein–DNA Binding and Transcription. *Acc. Chem. Res.* **2019**, *52*, 1730–1737. [CrossRef]
10. Reisacher, U.; Groitl, B.; Strasser, R.; Cserép, G.B.; Kele, P.; Wagenknecht, H.-A. Triazine-modified 7-deaza-2′-deoxyadenosines are better suited for bioorthogonal labelling of DNA by PCR than 2′-deoxyuridines. *Bioconjugate Chem.* **2019**, *30*, 1773–1780. [CrossRef]
11. Dziuba, D.; Jurkiewicz, P.; Cebecauer, M.; Hof, M.; Hocek, M. A Rotational BODIPY Nucleotide: An Environment-Sensitive Fluorescence-Lifetime Probe for DNA Interactions and Applications in Live-Cell Microscopy. *Angew. Chem. Int. Ed.* **2016**, *55*, 174–178. [CrossRef]

12. Güixens-Gallardo, P.; Humpolickova, J.; Miclea, S.P.; Pohl, R.; Kraus, T.; Jurkiewicz, P.; Hof, M.; Hocek, M. Thiophene-linked tetramethylbodipy-labeled nucleotide for viscosity-sensitive oligonucleotide probes of hybridization and protein–DNA interactions. *Org. Biomol. Chem.* **2020**, *18*, 912–919. [CrossRef] [PubMed]
13. Matyašovský, J.; Tack, L.; Palágyi, A.; Kuba, M.; Pohl, R.; Kraus, T.; Güixens-Gallardo, P.; Hocek, M. Nucleotides bearing aminophenyl- or aminonaphthyl-3-methoxychromone solvatochromic fluorophores for the enzymatic construction of DNA probes for the detection of protein–DNA binding. *Org. Biomol. Chem.* **2021**, *19*, 9966–9974. [CrossRef]
14. Tokugawa, M.; Masaki, Y.; Canggadibrata, J.C.; Kaneko, K.; Shiozawa, T.; Kanamori, T.; Grøtli, M.; Wilhelmsson, L.M.; Sekine, M.; Seio, K. 7-(Benzofuran-2-yl)-7-deazadeoxyguanosine as a fluorescence turn-ON probe for single-strand DNA binding protein. *Chem. Commun.* **2016**, *52*, 3809–3812. [CrossRef] [PubMed]
15. Schneider, A.F.L.; Hackenberger, C.P.R. Fluorescent labelling in living cells. *Curr. Opin. Biotechnol.* **2017**, *48*, 61–68. [CrossRef] [PubMed]
16. Bird, R.E.; Lemmel, S.A.; Yu, X.; Zhou, Q.A. Bioorthogonal Chemistry and Its Applications. *Bioconjugate Chem.* **2021**, *32*, 2457–2479. [CrossRef] [PubMed]
17. Crnković, A.; Vargas-Rodriguez, O.; Söll, D. Plasticity and Constraints of tRNA Aminoacylation Define Directed Evolution of Aminoacyl-tRNA Synthetases. *Int. J. Mol. Sci.* **2019**, *20*, 2294. [CrossRef]
18. Chung, C.Z.; Amikura, K.; Söll, D. Using Genetic Code Expansion for Protein Biochemical Studies. *Front. Bioeng. Biotechnol.* **2020**, *8*, 598577. [CrossRef] [PubMed]
19. Shandell, M.A.; Tan, Z.; Cornish, V.W. Genetic Code Expansion: A Brief History and Perspective. *Biochemistry* **2021**, *60*, 3455–3469. [CrossRef]
20. de la Torre, D.; Chin, J.W. Reprogramming the genetic code. *Nat. Rev. Genet.* **2021**, *22*, 169–184. [CrossRef]
21. Cserép, G.B.; Herner, A.; Kele, P. Bioorthogonal fluorescent labels: A review on combined forces. *Methods Appl. Fluoresc.* **2015**, *3*, 042001. [CrossRef]
22. Kozma, E.; Demeter, O.; Kele, P. Bio-orthogonal Fluorescent Labelling of Biopolymers through Inverse-Electron-Demand Diels-Alder Reactions. *ChemBioChem* **2017**, *18*, 486–501. [CrossRef]
23. Choi, S.-K.; Kim, J.; Kim, E. Overview of Syntheses and Molecular-Design Strategies for Tetrazine-Based Fluorogenic Probes. *Molecules* **2021**, *26*, 1868. [CrossRef]
24. Lipunova, G.N.; Nosova, E.V.; Zyryanov, G.V.; Charushin, V.N.; Chupakhin, O.N. 1,2,4,5-Tetrazine derivatives as components and precursors of photo- and electroactive materials. *Org. Chem. Front.* **2021**, *8*, 5182–5205. [CrossRef]
25. Armitage, B.A. Cyanine Dye–DNA Interactions: Intercalation, Groove Binding, and Aggregation. In *DNA Binders and Related Subjects*; Waring, M.J., Chaires, J.B., Eds.; Topics in Current Chemistry; Springer: Berlin/Heidelberg, Germany, 2005; pp. 55–76. ISBN 9783540314639.
26. Lartia, R.; Asseline, U. New Cyanine–Oligonucleotide Conjugates: Relationships between Chemical Structures and Properties. *Chem. Eur. J.* **2006**, *12*, 2270–2281. [CrossRef] [PubMed]
27. Ikeda, S.; Kubota, T.; Yuki, M.; Okamoto, A. Exciton-Controlled Hybridization-Sensitive Fluorescent Probes: Multicolor Detection of Nucleic Acids. *Angew. Chem. Int. Ed.* **2009**, *48*, 6480–6484. [CrossRef] [PubMed]
28. Suss, O.; Motiei, L.; Margulies, D. Broad Applications of Thiazole Orange in Fluorescent Sensing of Biomolecules and Ions. *Molecules* **2021**, *26*, 2828. [CrossRef]
29. Nguyen, S.S.; Prescher, J.A. Developing bioorthogonal probes to span a spectrum of reactivities. *Nat. Rev. Chem.* **2020**, *4*, 476–489. [CrossRef]
30. Meimetis, L.G.; Carlson, J.C.T.; Giedt, R.J.; Kohler, R.H.; Weissleder, R. Ultrafluorogenic Coumarin-Tetrazine Probes for Real-Time Biological Imaging. *Angew. Chem. Int. Ed.* **2014**, *53*, 7531–7534. [CrossRef] [PubMed]
31. Devaraj, N.K.; Hilderbrand, S.; Upadhyay, R.; Mazitschek, R.; Weissleder, R. Bioorthogonal Turn-On Probes for Imaging Small Molecules inside Living Cells. *Angew. Chem. Int. Ed.* **2010**, *49*, 2869–2872. [CrossRef]
32. Lee, Y.; Cho, W.; Sung, J.; Kim, E.; Park, S.B. Monochromophoric Design Strategy for Tetrazine-Based Colorful Bioorthogonal Probes with a Single Fluorescent Core Skeleton. *J. Am. Chem. Soc.* **2018**, *140*, 974–983. [CrossRef] [PubMed]
33. Bojtár, M.; Németh, K.; Domahidy, F.; Knorr, G.; Verkman, A.; Kállay, M.; Kele, P. Conditionally Activatable Visible-Light Photocages. *J. Am. Chem. Soc.* **2020**, *142*, 15164–15171. [CrossRef]
34. Bohländer, P.R.; Wagenknecht, H.-A. Bright and photostable cyanine-styryl chromophores with green and red fluorescence colour for DNA staining. *Methods Appl. Fluoresc.* **2015**, *3*, 044003. [CrossRef]
35. Dittmer, T.A.; Misteli, T. The lamin protein family. *Genome Biol.* **2011**, *12*, 222. [CrossRef]
36. Li, B.X.; Chen, J.; Chao, B.; Zheng, Y.; Xiao, X. A Lamin-Binding Ligand Inhibits Homologous Recombination Repair of DNA Double-Strand Breaks. *ACS Cent. Sci.* **2018**, *4*, 1201–1210. [CrossRef] [PubMed]
37. Kornberg, R.D.; Lorch, Y. Primary Role of the Nucleosome. *Mol. Cell* **2020**, *79*, 371–375. [CrossRef]
38. Kurumizaka, H.; Kujirai, T.; Takizawa, Y. Contributions of Histone Variants in Nucleosome Structure and Function. *J. Mol. Biol.* **2021**, *433*, 166678. [CrossRef] [PubMed]
39. Szatmári, Á.; Cserép, G.B.; Molnár, T.Á.; Söveges, B.; Biró, A.; Várady, G.; Szabó, E.; Németh, K.; Kele, P. A Genetically Encoded Isonitrile Lysine for Orthogonal Bioorthogonal Labeling Schemes. *Molecules* **2021**, *26*, 4988. [CrossRef] [PubMed]
40. Danielsson, F.; Peterson, M.; Caldeira Araújo, H.; Lautenschläger, F.; Gad, A. Vimentin Diversity in Health and Disease. *Cells* **2018**, *7*, 147. [CrossRef]

41. Endo, T.; Kohda, D. Functions of outer membrane receptors in mitochondrial protein import. *Biochim. Biophys. Acta Mol. Cell Res.* **2002**, *1592*, 3–14. [CrossRef]
42. Wurm, C.A.; Neumann, D.; Lauterbach, M.A.; Harke, B.; Egner, A.; Hell, S.W.; Jakobs, S. Nanoscale distribution of mitochondrial import receptor Tom20 is adjusted to cellular conditions and exhibits an inner-cellular gradient. *Proc. Natl. Acad. Sci. USA* **2011**, *108*, 13546–13551. [CrossRef]
43. Kozma, E.; Estrada Girona, G.; Paci, G.; Lemke, E.A.; Kele, P. Bioorthogonal Double-Fluorogenic Siliconrhodamine Probes for Intracellular Superresolution Microscopy. *Chem. Commun.* **2017**, *53*, 6696–6699. [CrossRef] [PubMed]